Distributed Fibre Optic Sensing and Adhesion Strategies for Strain Evaluation of an Aircraft Structure

Gerard Natividad [1], Suzana Turk [1], Kelly Tsoi [1] and Daniel Bitton [1]

[1] *Defence Science and Technology Group, 506 Lorimer Street, Fishermans Bend, Victoria, 3207, Australia*

Abstract

This paper reports on work demonstrating the repeatability and accuracy of a high-density strain measurement capability based on distributed fibre optic sensors (FOSs). Four FOS bonding strategies were experimentally validated on a large aircraft structure subjected to full scale fatigue testing under representative flight loading. Sensors were surface mounted using three different aerospace grade adhesives and an adhesive mesh tape. The strain measurements obtained under the different bonding methods were comparable, with key strain distribution features consistent. The FOS measurements were also compared at multiple locations to single point strain measurements from electrical resistance foil strain gauges, with good correlation demonstrated.

Keywords: fibre optic sensing, distributed strain measurement, fatigue testing, structural health monitoring

Introduction

Distributed fibre optic strain sensing based on draw tower grating (DTG) technology [1] can deliver high-density strain measurements. Fibre optic sensors (FOSs) are immune to electromagnetic interference, resistant to corrosion, have a high tensile fatigue failure strain and a small spatial footprint. These attributes make FOSs highly suitable for application in structural testing and for structural health monitoring (SHM). However, prior to implementation on operational aerospace platforms, further full-scale demonstration on geometrically complex aircraft structures is required to develop confidence in the method. Although it has been shown that FOSs are capable of withstanding high strain fatigue testing for extended periods on test coupons [2], there is uncertainty around the long-term reliability, repeatability, and accuracy of FOS strain measurement under combat aircraft loading conditions.

Additionally, most demonstrations of distributed sensing technologies based on Rayleigh and Brillion scattering and quasi-distributed fibre Bragg gratings (FBGs) have been limited to flat uniform structures such as aircraft wing surfaces [3-6]. In these studies FOSs were installed using foil strain gauge (FSG) bonding adhesives, which are susceptible to degradation by the effects of time, elevated temperature and moisture absorption. Another study evaluated packaged and direct surface-bonded discrete FBGs under axial load in environmental chambers to simulate in-flight environmental conditions [7]. Evaluation of fibre packaging and bonding using discrete FBGs limits the ability to characterise the influence of the packaging and adhesive material on strain distribution. Furthermore, the discrete FBG tests were carried-out on test coupons rather than geometrically complex structures where the fibre installation path is usually complicated and may need to traverse obstructions and sharp bends.

This paper compares strain measurements from distributed FOSs, installed using four adhesive packaging strategies, to FSG strain measurements on a geometrically complex aircraft component undergoing full-scale fatigue testing. Three aerospace grade adhesives were

selected based on their properties, which make them suitable for long-term aerospace applications such as peel strength, elongation and operating temperature range, Table 1.

Table 1: Adhesive properties and curing regime of aerospace adhesives and FSG adhesives for comparison

Adhesive	Bell Peel Strength (N/25 mm) @ Room Temperature	Tensile Strength (MPa)	Tensile Modulus (MPa)	Elongation (%)	Cure	Service Temperature (°C)
LOCTITE EA 9309.3NA AERO	396	31	2331	10	25°C/3-5 days or 82 °C/1 hr	71
LOCTITE EA 9394 AERO	89	46	4237	1.66	25°C/3-5 days or 93 °C/1 hr	177
LOCTITE EA 9396 AERO	111	35	2750	3.4	25°C/3-5 days or 66 °C/1 hr	-55 to 177
Micro-Measurements M-Bond AE-10	NA	NA	NA	6 to 10	24°C/6 hours	-195 to 95
Micro-Measurements M-Bond 200	NA	NA	NA	3	24°C/5 minutes	-32 to 65

Experimental Method

The fibre optic strain sensing system comprises All Grating Fibre (AGF) technology [1] and the Sensuron Summit (4 channel) Optical Frequency Domain Reflectometry (OFDR) interrogator [8]. The fibre is 3.25 m long and contains 2024 sensing points distributed uniformly at a 1.6 mm interval distance. Each FOS was bonded from the left to the right flange of the aircraft bulkhead, Fig.1. The location of the left and right flanges are expected to have load symmetry, which will provide another means of validating the strain profiles measured by the FOSs.

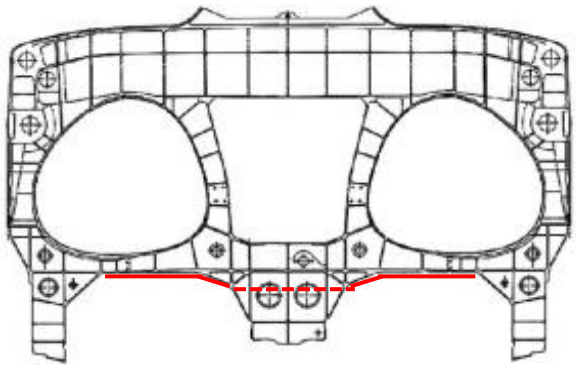

Fig. 1: Schematic of an aircraft bulkhead with FOS bonded positions indicated in solid red along the left and right flanges and unbonded FOS represented by the dashed red line

Three FOSs (FOS1 to FOS3) were surface bonded to the structure using four adhesive packaging strategies, Table 2. Airtech tac-strip mesh tape was used to immobilise FOS1,

provide good surface contact between the sensor and the structure, as well as to aid in controlling adhesive bond-line thickness. A thin film of epoxy adhesive encapsulated and bonded FOS2 and FOS3 to the flanges. Different adhesives were used to bond FOS3 on the left and right flanges.

Table 2: Installation approaches used for bonding three FOSs

Sensor	Adhesive	Installation method	Location
FOS 1	LOCITTE EA 9309.3NA AERO	Mesh tape & adhesive	LHS flange to RHS flange
FOS 2	LOCITTE EA 9309.3NA AERO	Adhesive only	LHS flange to RHS flange
FOS 3A	LOCITTE EA 9396 AERO	Adhesive only	LHS flange
FOS 3B	LOCITTE EA 9394 AERO	Adhesive only	RHS flange

Optical fibres have a minimum bending radius below which there is significant signal loss and the fibre breaks. Therefore, the fibre was unbonded in sections that required traversing of obstructions and sharp bends, such as when crossing brackets and stiffeners. These unbonded sections of FOS were protected within a plastic bridging sleeve, which was fixed in position using adhesive. Ingress and egress of optical fibre from bridging sleeves are prone to breakage and were therefore encapsulated with adhesive for protection.

As part of a structural assessment, the aircraft component underwent a full-scale fatigue test comprising multiple lifetimes of simulated flying hours (one lifetime is equivalent to ~6000 flying hours) with strains reaching 4000 με. Strain surveys were conducted routinely during the full-scale fatigue test to monitor FSG strain-drift. The FOS and FSG strain values corresponding to peak applied load during stepped strain survey load excursions were compared and evaluated. The strain responses corresponding to FOS1, FOS2 and FOS3 were recorded during separate strain surveys. Responses for FOS1 were recorded during the first simulated lifetime test after which the installation was removed and replaced with FOS2 and FOS3, which were installed in parallel along the same installation path as FOS1. The strain results for FOS2 and FOS3 were recorded during the second simulated lifetime test, which involved the same loading spectrum applied in the first test.

Results

The flange strain response measured by each FOS at peak load is shown in Fig. 2. The strain distribution graphs are aligned with a photo of the corresponding flange, in which features such as FSGs and intersecting stiffeners are labelled. Overall, there is excellent agreement between the strain distributions obtained from the FOSs that were implemented using the three installation methods. Importantly, significant strain features remain consistent across the different FOS installations. This includes the strain gradient along the flange as well as the location and magnitude of peak strain, which occur adjacent to FSG2A and FSG2B on both flanges.

Local strain variations were observed at various points on the FOS strain distribution graphs. Superimposing the position of stiffeners on the graph revealed a correlation between some strain variations and points on the flange intersected by stiffeners. Fig. 2 demonstrates symmetric strain profiles for the left and right-hand side flanges, as expected. Other factors such as changes in structure thickness also contribute to local strain variation, for example the local strain increase in the region located between FSG1A and FSG2A and FSG1B and FSG2B in Fig. 2. This demonstrates the value of the FOS high-density strain measurement capability

as these local strain variations occur over relatively short distances and are difficult to quantify using FSGs.

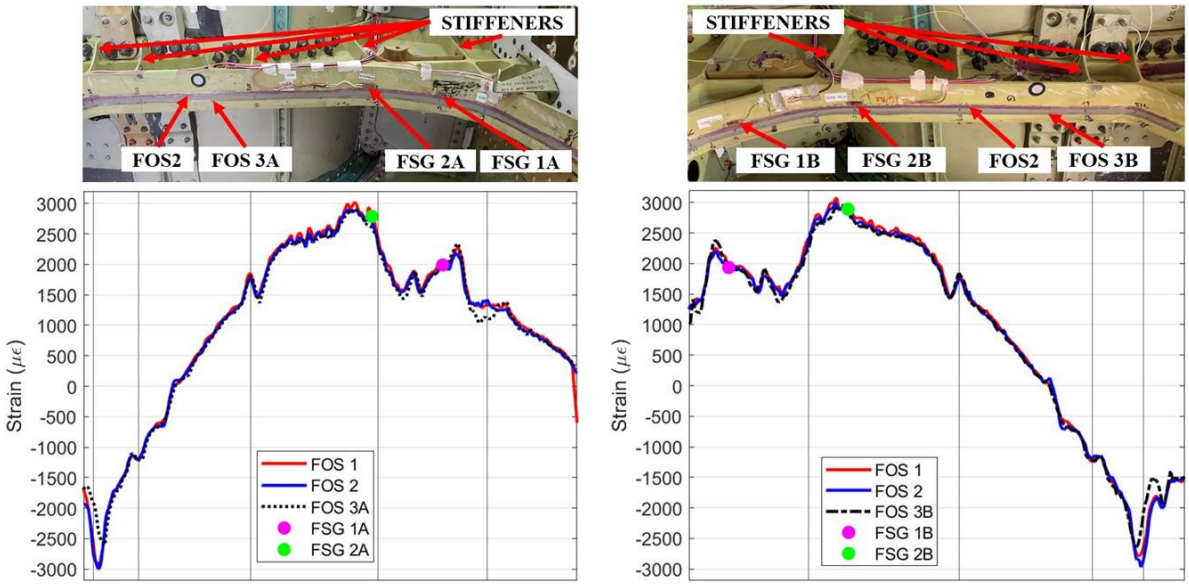

Fig. 2: Strain profiles of the left and right flanges obtained from three different FOS installations with stiffener-flange intersections (represented by vertical lines) and average FSG strain across three strain surveys

The consistency of the local strain fluctuations across the different sensor installations suggests these variations are real strain features rather than noise artefacts. The strain results obtained from FOS1 were reported in [9] and perturbations identified at some locations in the strain distribution, shown in Fig. 3, were surmised to be a combination of systematic noise and the cells of Airtech-tac strip mesh tape impinging on the fibre. After replacing FOS1 with FOS2 and FOS3 it was observed that the perturbations persisted at the same locations, Fig. 3. The perturbations measured by FOS1 and FOS2 show similar strain amplitudes, while those measured by FOS3 were smaller, but still noticeable. This difference in strain amplitudes might correspond to: non-uniform strain distribution across the width of the flange, FOS offset-distance from the centre of the flange with FOS3 being the furthest from the centre line, and/or local structural features near the centre of the flange. These possibilities are yet to be examined.

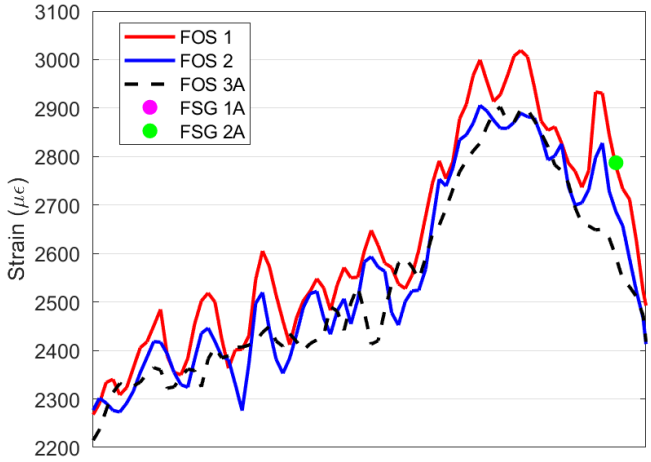

Fig. 3: Perturbations in the measured FOS strain profile of the left-hand side flange

The strain values measured by each of the FSGs vary slightly across the three strain surveys, the maximum variation being ~35 με. The difference between each FSG and corresponding

FOS strain value was calculated, with the values listed in Table 3. For example, the difference in strain between FOS1 and each of the FSGs range from 6 to 28 με. Since the FOSs are installed in parallel and offset by varying distances from the FSGs, some variation in strain is not unexpected. A greater strain deviation was observed between FOS3A and FSG2A. The location of FSG2A occurs near a local strain peak as measured by FOS1 and FOS2, Fig. 3. However, it was previously noted that the magnitude of local perturbations in measurements obtained by FOS3A were reduced, again possibly due to the offset distance, which may explain the greater comparative strain difference. Nevertheless, there is excellent agreement between the FSG strain values and the strain measurements obtained from each FOS.

Table 3: Difference in measured strain values between each FSG and FOS (values are in με)

	FOS1	**FOS2**	**FOS3A**	**FOS3B**
FSG1A	15	69	4	-
FSG2A	28	91	245	-
FSG1B	10	26	-	81
FSG2B	6	32	-	25
Strain range	6 – 28	26 – 91	4 – 245	

Conclusion

This paper has experimentally assessed four FOS bonding strategies which have been shown to yield comparable strain distribution measurements in a geometrically complex airframe component under full-scale fatigue testing. The high-density distributed FOS strain measurements provided information about the magnitude and location of peak strain and high strain gradients that is unavailable from FSGs. The adhered FOSs withstood one lifetime of simulated flying at strains up to 4000 με and are still operational and producing strain data for ongoing structural health monitoring activities.

All adhesive packaging strategies performed comparably. Adhesive selection depends on the application, environmental conditions and operational factors. Of the adhesives tested, Loctite EA9396 is recommended for its ease of use. The viscosity enables thin uniform adhesive application in any orientation, room temperature cure and a wide operating temperature range suited to the majority of aerospace applications.

Acknowledgements

The authors acknowledge the Structures and Materials Test Centre facility at DSTG and the technical assistance of Isaac Field and Keith Muller. The authors also acknowledge the collaborative opportunity provided by RMIT University, RUAG International and Armasuisse.

References

1. Information on https://fbgs.com/components/all-grating-fibers-agf/

2. N. Zhang, C. Davis, C.W. Kong and S. Turk, Trans-jacket fibre Bragg gratings for in-situ health monitoring of defence platforms in harsh environments. Materials Research Proceedings, 2021, vol. 18, doi:10.21741/9781644901311-6.

3. W. Lance Richards, A. Parker Jr, W. Ko, A. Piazza and P. Chan, Application of fibre optic instrumentation. NATO OTAN and Research and Technology Organisation (RTO), RTO AGARDograph 160, Flight Test Instrumentation Series-Volume 22, SCI-228, July 2012.

4. D. Wada and H. Igawa, Distributed fiber optic sensing for aircraft towards in-flight structural control. 27th International Conference on Optical Fiber Sensors, OSA, 2020.

5. R. Di Sante, Fibre optic sensors for structural health monitoring of aircraft composite structures: Recent advances and applications. Sensors, 15, 18666-18713, 2015. Doi: 10.3390/s150818666.

6. https://www.sensuron.com/lead-sensuron-technology-onboard-nasas-x-56-uav/

7. Goossens, S., De Pauw, B., Geernaert, T., Salmanpour, M. S., Sharif Khodaei, Z., Karachalios, E., Saenz-Castillo, D., Thienpont, H. and Berghmans, Francis., "Aerospace-grade surface mounted optical fibre strain sensor for structural health monitoring on composite structures evaluated against in-flight conditions", *Smart Materials and Structures*. Vol. 28, No. 6, 2019.

8. https://www.sensuron.com, Sensuron Summit technical data sheet.

9. Natividad, G., Turk, S., Tsoi, K. and Bitton, D., "Comparative Strain Survey of an Aerospace Structure Using Distributed Fibre Optic Strain Sensing Technology". Asia Pacific Workshop on Structural Health Monitoring, Cairns Australia, 2022.